

Study and Management of Bipolar LVDC Grid with DC Symmetrical Component Method

**Ramanaiah**

M.Tech Student
SSN Engineering College,
Ongole.



T Mahendra Reddy, M.Tech
Assistant Professor
SSN Engineering College,
Ongole.



K Sowjan Kumar, M.Tech
HoD
SSN Engineering College,
Ongole.

Abstract

The power distribution network will be changed towards the future Smart Grid due to increased number of installed renewable power generation units to fulfill the tightened environmental regulation. The control of the future Smart Grid will be challenging due to increased number of renewable power generation units, which are variable in nature, and at the same time, the customers are highly dependent on uninterruptable, high quality power supply. The Smart Grid control is intensively studied. It can be concluded that the control might be simpler and the grid operation more reliable if the AC grid would be replaced by DC grid. However, the detailed energy efficiency analysis of the DC grid is not thoroughly studied. The efficiency and total lifetime costs are the key parameters when the network owners consider the future grid structure.

INTRODUCTION

This thesis addresses the factors, which affect the energy efficiency of the low voltage DC (LVDC) distribution network from power electronics perspective. The power loss models for the converters and their AC filters are developed and verified by measurements. The impact on the converter topology, used power semiconductor switches, AC filter design and inductor core material, DC network configuration, customer behavior, the need of DC voltage balancing in the bipolar DC network as well as the grounding issues

to fulfill the electrical safety standards are treated. For facilitating the design of cost effective LVDC distribution networks, the total power losses of the network with different configurations are evaluated and compared.

It is revealed that the used filter inductor core material has a significant impact on the power losses of the LVDC distribution network. The inductor core material having low high-frequency power loss characteristics, such as amorphous alloy, is recommended. The LVDC distribution network should be grounded to minimize the power losses whenever it is possible according to the local safety standardization and grounding conditions. The three-level NPC converters connected to 1500 VDC should be used to minimize the power losses. The grid-frequency isolation transformer is the main power loss source if the galvanic isolation is needed to isolate the ungrounded LVDC distribution network and the grounded customer electrical installations.

In this case, the highest energy efficiency is achieved by using two- or three-level converters connected to 750 VDC if the DC cable length is less than 600 m. Otherwise, slightly higher energy efficiency is achieved by using three-level converters connected to 1500 VDC. Therefore, voltage transformation ratio of the isolation transformer must be 800V/400V instead of 400V/400V.

Moreover, the efficiency of the power converters is increased by using SiC MOSFETs instead of conventional IGBTs as power semiconductor switches.

The dc symmetrical component method is introduced for the analysis and control of bipolar dc distribution systems under asymmetrical operation. This method is an extension of the classical symmetrical component theory in three-phase ac power systems. As an example, an enhanced common-mode voltage regulation scheme is described.

It suppresses common-mode LC resonance by adding active damping control, and reduces common-mode impedance to improve power quality and voltage stability. DC power delivery is regaining popularity recently after it was temporarily defeated by its ac opponent a century ago. The most significant development was found in high voltage dc (HVDC) transmission systems, due to its advantage in power capacity and controllability over ac transmission lines.

Now the trend of dc is expanding to the bottom part of the electrical supply chains, from transmission to distribution systems. It is foreseen that dc distribution may help to accommodate a higher penetration of renewable distributed generators (DGs), increase power capacity and quality, and provide greater resilience against power surge and irregular loads. The exploration of dc distribution technologies begins at the lowest voltage level. The major reason is the relative maturity of low-voltage dc (LVDC) electric apparatus, including power electronic converters and dc circuit breakers.

Primary dc distribution systems are first deployed for communication power supplies, with a rated voltage of only 48 V [11]. This is followed by transportation power systems, such as those in more electric aircrafts and ships. Correspondingly, the dc voltage level is scaled up to several hundred volts to handle the extended power range. The latest dc distribution initiatives are also reaching for residential applications in green buildings and electric vehicle charging stations.

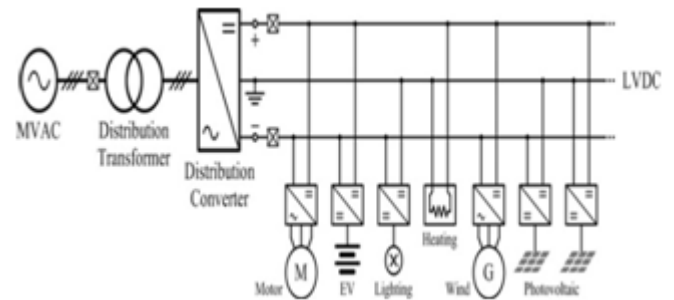


Fig.1. Bipolar LVDC Power Distribution System.

A typical LVDC grid is shown in Fig. 1. A distribution converter combined with a distribution transformer acts as the interface between the mid-voltage ac (MVAC) and LVDC grid. Just like the three-phase structure in ac power systems, a bipolar configuration can be adopted for the dc grid to provide two alternative voltage levels for DGs and loads with different voltage or power scales [10], [11]. The voltage between the positive and negative poles is similar to the line-line voltage in three-phase systems, while each pole is analogous to a single phase to provide a lower voltage for smaller equipment. One of the major challenges for a bipolar dc grid is the asymmetrical operation caused by the uneven power distribution in the two poles. Such asymmetry may lead to voltage unbalance, and deteriorate power quality and voltage stability. To deal with this problem, a comprehensive investigation is needed in both the converter topology and the operation control strategy. In this paper, the dc symmetrical component method is introduced for analysis and control of bipolar dc distribution systems.

This approach uses a similar methodology and provides a similar benefit to that of the classical ac symmetrical component theory [2]–[6]. The asymmetrical voltage and current of each pole are decomposed into symmetrical components in common mode and differential mode. Then the equivalent circuit for each mode can be derived, which turns out to be decoupled. Consequently, it provides an insightful view of the static and dynamic behavior of bipolar dc power systems, and simplifies the operation analysis and design. As an application of the introduced method, an

enhanced common-mode voltage regulation scheme is developed for a LVDC distribution system. It provides effective damping of the possible common-mode voltage oscillation, and offers tight voltage balance control by reducing the common-mode impedance. The proposed technique is also suitable for more sophisticated bipolar dc distribution systems with multiple sources and complex grid structures. Moreover, the extensive research works initially targeted on a unipolar dc distribution grid can be readily migrated to a bipolar grid, taking advantage of the symmetrical component decomposition and decoupling [7]– [10]. The paper is organized as follows. Section II gives an introduction to the bipolar LVDC converter topologies, to lay the physical basis for the analysis throughout this paper.

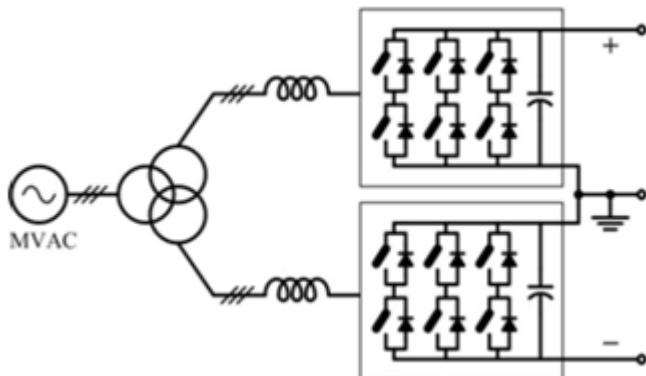


Fig.2. Bipolar LVDC Distribution Converter with Two Cascaded VSCS.

BIPOLAR LVDC DISTRIBUTION CONVERTER TOPOLOGIES

The distribution converter is the power hub of the entire LVDC grid. In this section, the converter topologies suitable for bipolar LVDC distribution are briefly summarized. They are the physical bases for the theoretical derivation in succeeding sections. The most straightforward approach to build a converter with bipolar dc output is to use two cascaded voltage source converters (VSCs), as shown in Fig. 2. This topology essentially contains two independent voltage sources, and therefore permits independent operation of the positive and negative poles. However, two separated converters are needed in such a configuration, along

with two isolated windings in the distribution transformer. This may result in increased size and cost.

Bipolar dc voltage can also be acquired by a single VSC with some modifications. For example, the neutral line of the transformer can be connected to the mid-point of the dc output capacitors, as depicted in Fig. 3. The current in the neutral line can be regulated to balance the dc side voltage. Unfortunately, the neutral line current may contain significant dc component in this case, which should be strictly limited to prevent transformer saturation. In order to prevent the neutral line dc current, an extra half bridge can be employed, which is dedicated to voltage balancing by actively redistributing the currents, as displayed in Fig.3.

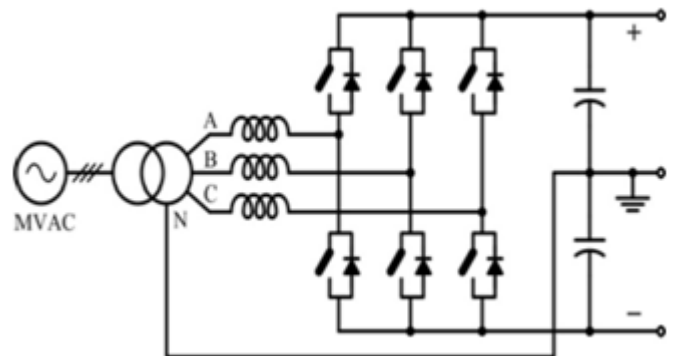


Fig.3. VSC with Neutral Line Connected to Dc Mid-Point.

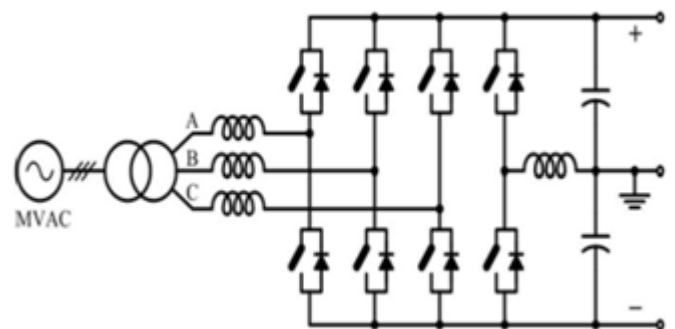


Fig.4. VSC with Extra Voltage Balancing Half Bridge.

This topology provides greater tolerance of unbalanced load currents than Fig. 3, and also has a simplified structure compared with Fig. 4. Therefore, it is adopted in this paper as the distribution converter to power the bipolar LVDC grid.

In Fig. 4, the positive and negative poles are not independent, and therefore may induce the interaction between each pole. A method is needed to precisely model the possible inter-pole interference in bipolar dc systems. The dc symmetrical component method provides an effective solution to this problem, which is presented in the following section.

SV-PWM

As would be clear from the discussions in the above sections, the SV-PWM is concerned with the control of inverter output voltages in a unified manner. It does not control the individual phase voltages separately. The instantaneous magnitude and direction of the desired resultant voltage vector is decided as per the frequency and magnitude of inverter's fundamental output voltage. The SV-PWM is best realized with the help of a digital computing device, like microprocessor or Digital Signal Processor. The algorithm to be executed is outlined below:

Get the input data like; input dc link voltage (E_{dc}), desired output frequency „ f_{OP} “ (this will determine the speed of the resultant voltage vector), desired phase sequence of output voltage (will determine which way, clockwise or anticlockwise, the resultant voltage vector is moving), desired magnitude of output voltage and the desired switching frequency. It will be shown later that the switching frequency (f_{sw}) and sampling time period (T_s) are related. During each sampling time period three switching take place, where one turn-on and one turn-off is taken as one switching.

- Get the input data like; input dc link voltage (E_{dc}), desired output frequency ' f_{OP} ' (this will determine the speed of the resultant voltage vector), desired phase sequence of output voltage (will determine which way, clockwise or anticlockwise, the resultant voltage vector is moving), desired magnitude of output voltage and the desired switching frequency. It will be shown later that the switching frequency (f_{sw}) and sampling time period (T_s) are related. During each sampling time period three switching take place, where one turn-on and one turn-off is taken as one switching.

- Calculate magnitude factor ' α ' from the knowledge of input dc link voltage and the desired output voltage ($\alpha E_{dc} = 3/2$ times peak of phase voltage). Also, calculate the sampling time period $T_s = 1/(3 f_{sw})$.
- Initialize sector position = I, and angle ' θ ' = 0. Assume the rotating space voltage vector to remain stalled at this position for the sampling time period ' T_s '. Calculate the time duration for active and null state vectors as per Eqns. (38.4) to (38.6). Output the inverter switching pulses as per the calculated time durations so as to realize the space vectors in the following sequence: $V_8(111), V_1(101), V_2(100), V_7(000)$.
- Calculate the next position angle $SOPold2Tf\theta = \pi + \theta$ for clockwise rotation in the vector space-plane of Fig. 38.4. The reader should be able to work out the changes when the rotation is anti-clock wise. Recalculate the time durations as in step (3) above but this time the switching sequence will be $V_7(000), V_2(100), V_1(101), V_8(111)$.
- Step (4) is to be repeated but every time the switching sequence alternates between the sequences given in steps 4 and 5. This helps in reducing the switching losses. The reader may note that this way there are only 3 switching per sampling period. The switching to next space vector involves change of only one bit of the switching word (i.e., only one turn-on and one turn-off). When the space vector enters sector-II (for), the vector $V_1/3\theta \geq \pi$ is replace by V_2 and V_2 is replaced by V_3 . At the same time, angular position is reset to a value within by subtracting 60 degrees from the old value. Every time the voltage vector enters a new sector the angle θ is readjusted so that it varies between 0 and 60 degrees. The active state vectors are also reassigned as described above. The process continues to produce a continuously rotating voltage space vector of fixed magnitude and fixed speed.

The ac output voltage produced by the VSI of a standard ASD is a three-level waveform. Although this waveform is not sinusoidal as expected its fundamental component behaves as such. This behavior should be ensured by a modulating technique that controls the amount of time and the sequence used to switch the power valves on and off. The modulating techniques most used are the carrier-based technique (e.g.,

sinusoidal pulse width modulation, SPWM), the space-vector (SV) technique, and the selective-harmonic-elimination (SHE) technique. Three-leg voltage source inverter is because of the constraint that the input lines must never be shorted and the output current must always be continuous a voltage source inverter can assume only eight distinct topologies. Six out of the eight topologies produce a nonzero output voltage and are known as non-zero switching states and the remaining two topologies produce zero output voltage and are known as zero switching states. Space vector modulation (SVM) for three-leg VSI is based on the representation of the three phase quantities as vectors in a two-dimensional plane in Fig. 3. We see that the line voltages V_{ab} , V_{bc} , and V_{ca} are given by

$$\begin{aligned} V_{ab} &= V_s & (1) \\ V_{bc} &= 0 & (2) \\ V_{ca} &= -V_s & (3) \end{aligned}$$

This can be represented in the α, β plane as shown in Figure 4, where voltages V_{ab} , V_{bc} , and V_{ca} are three line voltage vectors displaced by 120 in space [6]. The effective voltage vector generated by this topology is represented as $V_1(pnn)$ in Figure 4. Here the notation „pnn“ refers to the three legs/phases a, b, c being either connected to the positive dc rail (p) or to the negative dc rail (n). Thus „pnn“ corresponds to „phase a“ being connected to the positive dc rail and phase b and c being connected to the negative dc rail. Space Vector PWM supplies the AC machine with the desired phase voltages. The SVPWM method of generating the pulsed signals fits the above requirements and minimizes the harmonic contents. Note that the harmonic contents determine the copper losses of the machine which account for a major portion of the machine losses.

Taking into consideration the two constraints quoted above there are eight possible combinations for the switch commands. These eight switch combinations determine eight phase voltage configurations. The vectors divide the plan into six sectors. Depending on the sector that the voltage reference is in, two adjacent vectors are chosen.

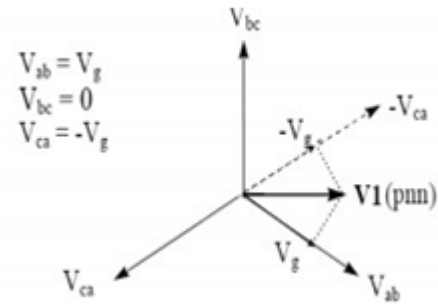


Fig.5. Topology 1-V1 (Pnn) of a Voltage Source Inverter

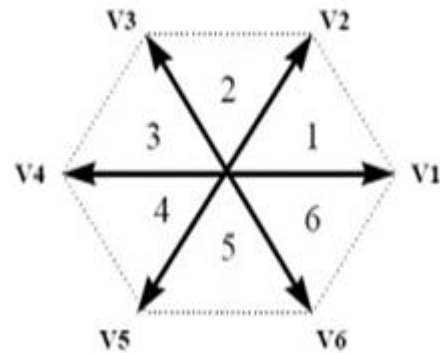


Fig.6. Representation of Topology 1 in the A, B Plane

Proceeding on similar lines the six non-zero voltage vectors ($V_1 - V_6$) can be shown to assume the positions shown in Fig.5. The tips of these vectors form a regular hexagon. We define the area enclosed by two adjacent vectors, within the hexagon, as a sector. Thus there are six sectors numbered 1 - 6 in Fig. 6 Fig. 6 Non-zero voltage vectors in the α, β plane.

A. Comparison of Sinusoidal and Space Vector PWM

The SVPWM generates minimum harmonic distortion of the currents in the winding of 3-phase AC motor. SV Modulation also provides a more efficient use of the supply voltage in comparison with sinusoidal modulation methods. In fact, with conventional sinusoidal modulation [1],[7],[8] in which the sinusoidal signals are compared with a triangular carrier, we know that the locus of the reference vector is the inside of a circle with a radius of $1/2 V_{DC}$. In the SV modulation it can be shown that the length of each of the six vectors is $2/3 V_{DC}$. In steady state the reference vector

magnitude might be constant. This fact makes the SV modulation reference vector locus smaller than the hexagon described above. This locus narrows itself to the circle inscribed within the hexagon, thus having a radius of $1/3V_{DC}$. In Fig. 6 below the different reference vector loci are presented.

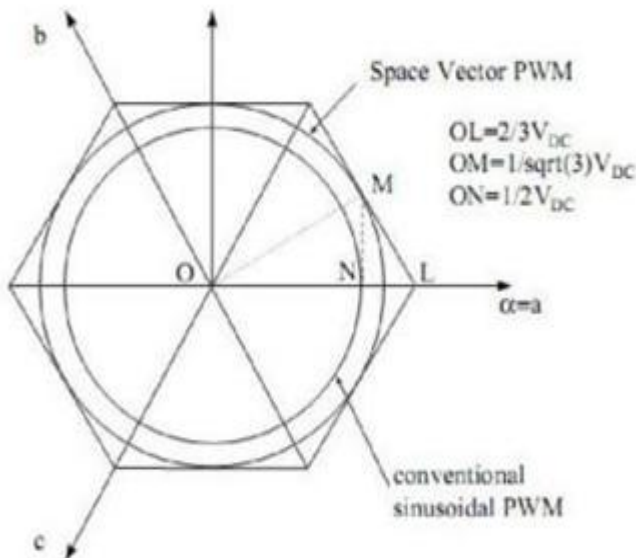


Fig.7. Locus Comparison SV-Sinusoidal PWM

Therefore, the maximum output voltage based on the Space Vector theory is $1.15OM/ON$ times as large as that of the conventional sinusoidal modulation. This explains why, with SVPWM, we have a more efficient use of the supply voltage than with the sinusoidal PWM method. Machine equations are converted in the rotor flux frame. Rotor flux is turning in synchronous speed but in a different angle than stator flux, if there is a sinusoidal excitation. Choosing d-axis on the rotor flux, q component will be zero. This fact simplifies the equations very much.

This method is very similar to DC machine's independent excitation where flux is the function of field current and torque is in proportion with flux and rotor current. The main problem of vector control method is flux axis angle calculation where is done by measuring the flux in two points with 90 degrees displacement and then angles are calculated using the resulted fluxes or estimating in regard to rotor speed [9].

SIMULATION RESULTS

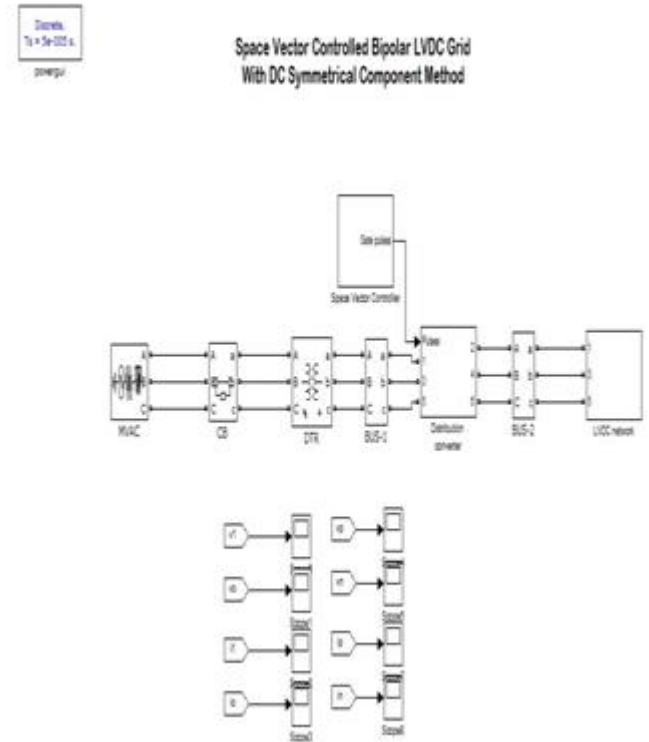
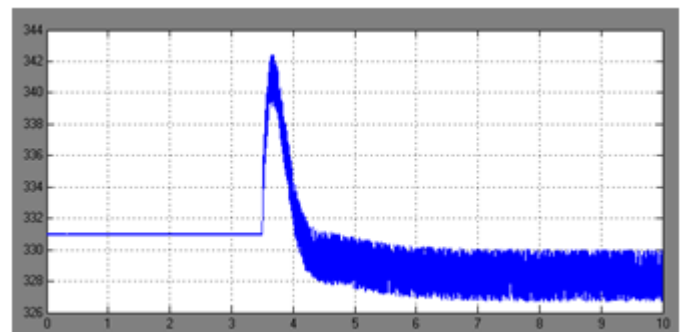
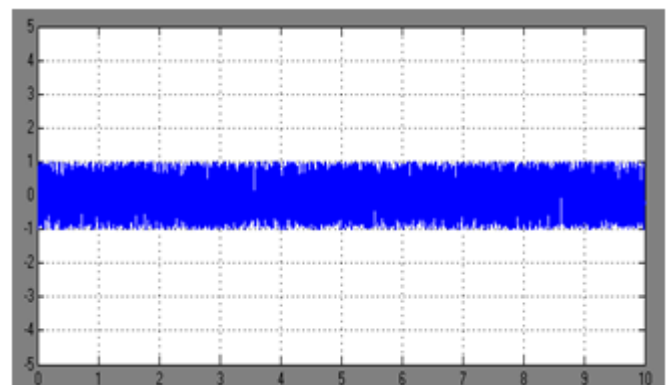


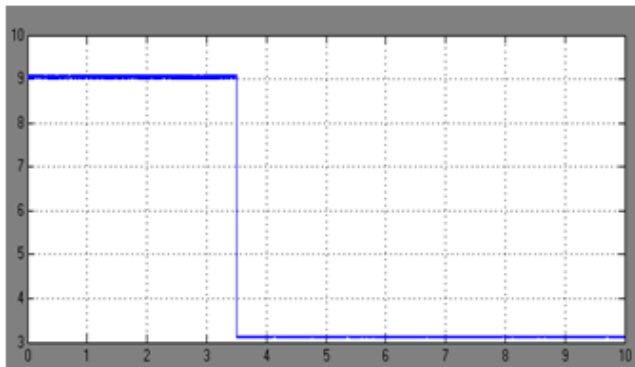
Fig.8. Circuit



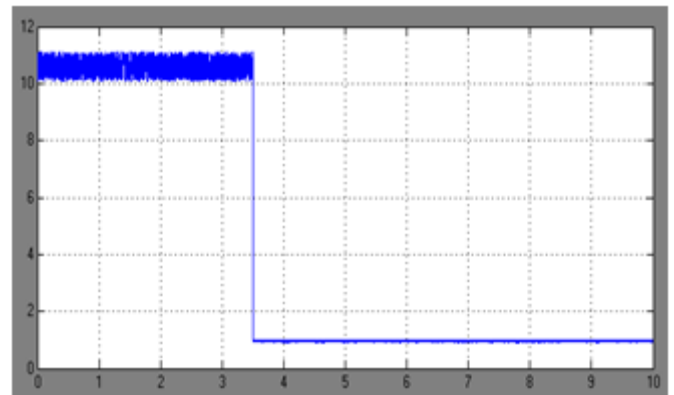
(a) V1



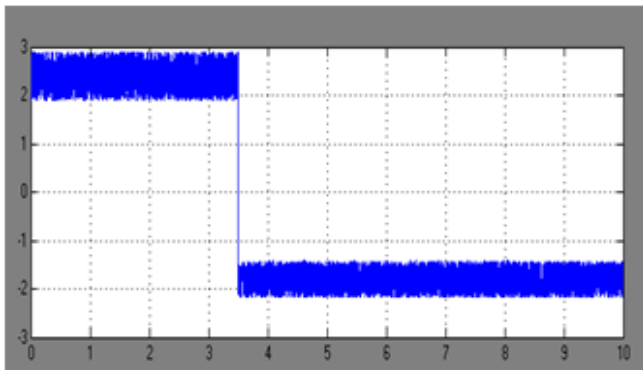
(b) Vo



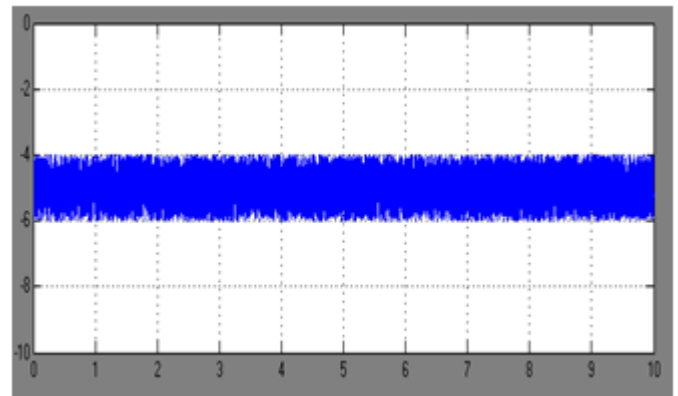
(c) I_i



(c) I_p



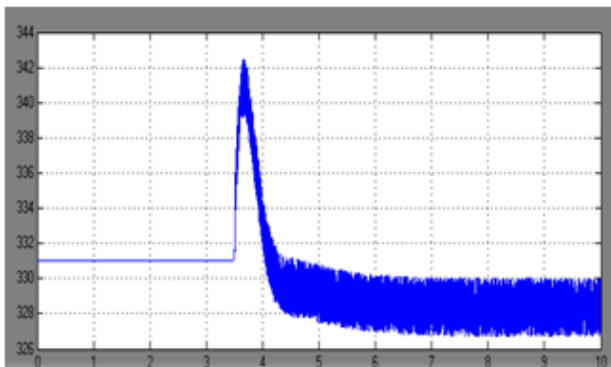
(d) I_0



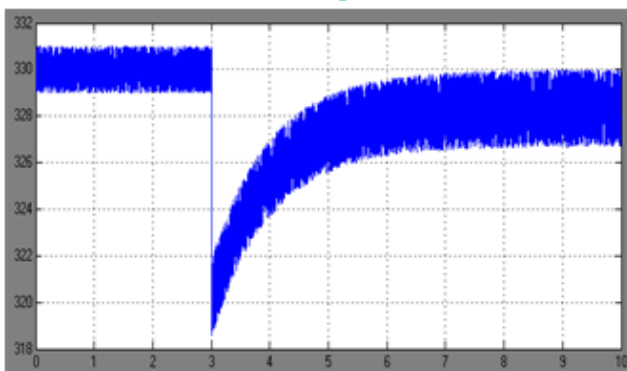
(d) I_n

Fig.9. Mode Voltage and Current

Fig.10. Pole Voltage and Current.



(a) V_p



(b) V_n

CONCLUSION

The dc symmetrical component method provides a useful tool for the analysis and control of bipolar LVDC distribution systems. It decomposes a bipolar dc grid into decoupled differential-mode and common-mode networks, thereby enabling separated and simplified investigation of each mode. Based on this method, the enhanced common-mode voltage regulation scheme shows advantageous performances in damping the common-mode LC resonance to improve power quality and voltage stability.

REFERENCE

- [1] Yunjie Gu, Wuhua Li, Member, IEEE, and Xiangning He, Fellow, IEEE "Analysis and Control of Bipolar LVDC Grid With DC Symmetrical Component Method" IEEE TRANSACTIONS ON POWER SYSTEMS, VOL. 31, NO. 1, JANUARY 2016.

- [2]M. E. Baran and N. R. Mahajan, “DC distribution for industrial systems: opportunities and challenges,” *IEEE Trans. Ind. Applicat.*, vol. 39, pp. 1596–1601, 2003.
- [3]K. Strunz, E. Abbasi, and D. N. Huu, “DC microgrid for wind and solar power integration,” *IEEE J. Emerg. Select. Topics Power Electron.*, vol. 2, pp. 115–126, 2014.
- [4]X. Feng, J. Liu, and F. C. Lee, “Impedance specifications for stable DC distributed power systems,” *IEEE Trans. Power Electron.*, vol. 17, pp. 157–162, 2002.
- [5]F. C. Lee, P. Barbosa, X. Peng, Z. Jindong, B. Yang, and F. Canales, “Topologies and design considerations for distributed power system applications,” *Proc. IEEE*, vol. 89, pp. 939–950, 2001.
- [6]Z. He, F. Mollet, C. Saudemont, and B. Robyns, “Experimental validation of energy storage system management strategies for a local DC distribution system of more electric aircraft,” *IEEE Trans. Ind. Electron.*, vol. 57, pp. 3905–3916, 2010.
- [7]J. G. Ciezki and R. W. Ashton, “Selection and stability issues associated with a navy shipboard DC zonal electric distribution system,” *IEEE Trans. Power Del.*, vol. 15, pp. 665–669, 2000.
- [8]G. Byeon, T. Yoon, S. Oh, and G. Jang, “Energy management strategy of the DC distribution system in buildings using the EV service model,” *IEEE Trans. Power Electron.*, vol. 28, pp. 1544–1554, 2013.
- [9]B. Sanzhong, D. Yu, and S. Lukic, “Optimum design of an EV/PHEV charging station with DC bus and storage system,” in *Proc. IEEE Energy Conversion Congr. Expo. (ECCE)*, 2010, pp. 1178–1184.
- [10]H. Kakigano, Y. Miura, and T. Ise, “Low-voltage bipolar-type DC microgrid for super high quality distribution,” *IEEE Trans. Power Electron.*, vol. 25, pp. 3066–3075, 2010.
- [11]J. Lago and M. L. Heldwein, “Operation and control- oriented modeling of a power converter for current balancing and stability improvement of DC active distribution networks,” *IEEE Trans. Power Electron.*, vol. 26, pp. 877–885, 2011.
- [12]G. C. Paap, “Symmetrical components in the time domain and their application to power network calculations,” *IEEE Trans. Power Syst.*, vol. 15, pp. 522–528, 2000.
- [13]M. Karimi-Ghartemani and H. Karimi, “Processing of symmetrical components in time-domain,” *IEEE Trans. Power Syst.*, vol. 22, pp. 572–579, 2007.
- [14]F. J. Alcantara and P. Salmeron, “A new technique for unbalance current and voltage estimation with neural networks,” *IEEE Trans. Power Syst.*, vol. 20, pp. 852–858, 2005.
- [15]T. Jen-Hao, “Unsymmetrical short-circuit fault analysis for weakly meshed distribution systems,” *IEEE Trans. Power Syst.*, vol. 25, pp. 96–105, 2010.
- [16]A. G. Phadke, M. Ibrahim, and T. Hlibka, “Fundamental basis for distance relaying with symmetrical components,” *IEEE Trans. Power App. Syst.*, vol. PAS-96, pp. 635–646, 1977.
- [17] R. W. Erickson and D. Maksimovic, *Fundamentals of power electronics*, 2nd ed. Norwell, MA, USA: Kluwer, 2001.
- [18]D. Pan, X. Ruan, C. Bao, W. Li, and X. Wang, “Capacitor-current-feedback active damping with reduced computation delay for improving robustness of LCL-type grid-connected inverter,” *IEEE Trans. Power Electron.*, vol. 29, pp. 3414–3427, 2014.